Development of a Smart Lung Health Monitoring System Using Sensors and Data Analytics for Early Disease Detection

Gulnur Tyulepberdinova[1], Murat Kunelbayev[2], Gulshat Amirkhanova[3], Meruyert Sakypbekova[4,*], Saltanat Adilzhanova[5], Ardak Tolepberdinova[6]

[1,2,3,4,5,6]*Department of Artificial Intelligence and Big Data, Al-Farabi Kazakh National University, Almaty, Kazakhstan*

(Received: March 01, 2025; Revised: May 13, 2025; Accepted: July 25, 2025; Available online: September 01, 2025)

Abstract

This study introduces a novel multimodal wearable sensor system for real-time monitoring and analysis of respiratory and cardiac activity. The primary objective is to facilitate the early detection of cardiopulmonary abnormalities by integrating electrical (ECG) and acoustic data. A total of 30 participants, aged 25 to 50 years, were involved in controlled breathing experiments, which included deep (1000 ml, 15 breaths/min), moderate (750 ml, 20 breaths/min), and shallow (500 ml, 30 breaths/min) breathing, as well as coughing simulations. Signal processing using a 7th-order polynomial approximation yielded the lowest modeling error at 6.8%, ensuring precise waveform reconstruction. The system demonstrated a clear differentiation of respiratory patterns via Area Under the Curve (AUC) metrics, with average AUC values increasing from 1200 µV·s during shallow breathing to 3200 µV·s during deep breathing. Further analysis of the first derivative of AUC values revealed a strong correlation (r = 0.89) between respiratory volume and ECG amplitude fluctuations, highlighting robust cardiorespiratory coupling. Notably, the system achieved a 92% accuracy in detecting abnormal breathing events, such as shallow breathing and coughing fits. By combining ECG-derived heart rate variability with respiratory data, the system offers a comprehensive assessment of cardiopulmonary interaction. The key contribution of this work lies in its real-time, continuous monitoring capability using a compact wearable form factor, which distinguishes it from existing single-modality systems. This approach represents a significant advancement in non-invasive health monitoring, with strong potential for application in clinical diagnostics and home-based tracking of chronic conditions, such as asthma, COPD, and cardiac dysregulation.

Keywords: Biomedical Signal Processing, Wearable Sensor Data Analytics, Multimodal Data Fusion, Respiratory Pattern Classification, ECG Signal Analysis, Time-Series Feature Extraction, Digital Health Monitoring, Real-Time Health Data Analysis, Cardiopulmonary Interaction Modeling, Machine Learning In Healthcare

1. Introduction

Research [1], [2] shows that recent advances in environmental monitoring sensors and physiological parameters, as well as signal processing and machine learning, open up new prospects for improving the quality of life of people with chronic diseases. These technologies not only improve health monitoring but also provide valuable information for the scientific community, contributing to the development of advanced diagnostic and monitoring methods. The study [1], [2] also shows that for effective analysis, treatment, and reduction of negative effects on health, it is necessary to use synchronized devices such as smartphones, tablets, and laptops, which allow combining data and devices into closed control systems, including the concept of "man in a cycle". The advantage of intelligent wearable devices is the ability to remotely monitor and diagnose without being tied to stationary laboratory equipment that requires an electrical connection. Modern health monitoring systems process multidimensional biomedical data in real-time with high resolution, and personalized monitoring models allow for taking into account individual user characteristics, which increases diagnostic accuracy. The work [3], [4] shows that before the COVID-19 pandemic, chronic respiratory diseases were the third leading cause of death in the United States. One of the most common conditions is asthma, which affects 18.7 million adults (8%) and 6.8 million children (9.3%). These indicators underscore the need to develop effective systems for monitoring and managing respiratory diseases, particularly in settings with an increased risk of infectious complications. Research [5] shows that traditional clinic visits remain a key method for assessing the

***Corresponding author: Meruyert Sakypbekova (sakypbekova.meruyert@gmail.com)**
DOI: https://doi.org/10.47738/jads.v6i4.857

condition of patients with asthma, as well as identifying possible environmental triggers related to the disease. However, the effectiveness of treatment increases significantly with the use of complex therapeutic approaches, including individualized self-management and joint decision-making by doctors and patients. This approach helps to increase adherence to therapy and improve disease control. Personalized medicine requires effective methods to identify asthma triggers and factors that worsen the disease. Remote monitoring systems enable the development of individualized treatment plans, enhancing patient adherence to therapy and ultimately improving clinical outcomes [6]. This study has developed a wearable multimodal wireless sensor device designed for continuous real-time breath analysis. A sensor placed in the chest area records respiratory episodes (for example, cough) and physiological parameters (heart rate and respiration). Additionally, machine learning algorithms are employed to detect respiratory disorders and categorize the severity of respiratory symptoms. The results of this study complement the existing work in the field of remote respiratory monitoring, previously presented by various research groups. In [7], [8], it is demonstrated that inertial measuring devices mounted on the chest and abdomen make it possible to analyze respiratory cycles and patterns. This approach ensures continuous monitoring of respiratory activity and can be useful for diagnosing respiratory disorders. Studies have shown that low-power nanosensors, such as humidity sensors, can effectively monitor respiratory processes [9]. Soft electronics applied to the skin enable the recognition of human movements related to breathing [10]. Accurate measurement of respiratory volume plays a crucial role in diagnosing respiratory diseases, and bioimpedance measurement is widely used to assess lung volume [11]. In [12], a combined method was proposed, incorporating the analysis of breathing sounds and an Electromyogram (EMG) recorded from the diaphragm muscles, which enables the estimation of respiratory volume. However, this method is effective only for measurements near the respiratory muscles. One of the most common methods of early detection of respiratory disorders is the analysis of breathing sounds, which are closely related to the cycles of heartbeat and respiration [13], [14]. Studies [15], [16], [17], [18], [19], [20] have shown that the respiratory signal can be extracted from an ECG using various methods. One approach involves analyzing ECG variations to quantify respiratory movements. Another common method is based on measuring the heart rate through the analysis of RR intervals, which are affected by respiratory sinus arrhythmia (RSA). This method is most effective for young and healthy people, in whom RSA is more pronounced. In addition, the heart rate increases during inspiration and decreases during exhalation [21]. This study proposes a novel approach to remotely monitoring lung conditions using a wearable sensor device that integrates ECG measurements and breathing sounds. This method enables the detection of changes in lung function by analyzing both signals. The combination of breathing sounds and their physiological effects on the cardiovascular system can significantly improve the accuracy of modeling respiratory episodes such as shortness of breath and cough. Modern advances in materials, structures, and integration technologies offer improved sensor-wearing comfort. However, to develop truly effective and clinically relevant wearable devices, several technical problems must be addressed, including long-term respiratory monitoring, energy consumption optimization, data storage, wireless information transmission, and automated diagnostics [1].

2. Methods

The developed lung health monitoring system is designed for continuous monitoring of respiratory function based on the analysis of acoustic and electrophysiological signals. As part of the study, experimental measurements were conducted to evaluate the accuracy and effectiveness of the proposed system in comparison with traditional methods for diagnosing respiratory diseases.

As part of the study, a lung health monitoring system was developed, including a piezoelectric sensor, a MEMS microphone, and a differential ECG sensor for recording acoustic and electrophysiological respiratory signals. The data was processed using an STM32 microcontroller and transmitted via Bluetooth Low Energy (BLE) to a personal computer for analysis in MATLAB. Experiments were conducted using different breathing modes, including deep, moderate, shallow, and asthmatic cough. The recorded signals were filtered and analyzed to identify respiratory patterns, assess respiratory rate, and amplitude characteristics. The results were compared with standard diagnostic methods such as spirometry.

The scientific novelty of this study is the creation of a lung health monitoring system that integrates a piezoelectric sensor with an integrated amplifier and a multichannel differential ECG sensor for accurate and comprehensive collection of physiological data. The transmitted signals are processed and analyzed using the STM32 microcontroller,

which provides detailed diagnostics and real-time data processing. The sound recording module is equipped with a microelectromechanical system for capturing acoustic characteristics of breathing and other sound phenomena, which significantly expands the diagnostic capabilities of the system. An integrated chip featuring an amplifier and an analog-to-digital converter is utilized for signal processing, enabling the conversion and encoding of analog signals into digital form with minimal loss. Bluetooth Low Energy technology is used for wireless data transmission, which provides low power consumption and reliable data transmission to a personal computer for further analysis and interpretation. This technology enables the system to automatically upload patient status data to medical information systems, enhancing the interaction between medical institutions and healthcare providers. Two textile electrodes are used for ECG recording, which have been adapted and integrated into a system designed to improve diagnostic efficiency and enhance interaction between medical institutions and patients. The result of signal processing in an external computer system is the classification of signs for making clinical diagnostic decisions, such as respiratory volume during normal breathing and abnormal cough.

The system utilizes BLE for wireless communication between the wearable device and the host computer. The average data transmission latency was measured at 25–40 ms, which is sufficient for quasi-real-time monitoring of respiratory parameters. The effective data rate ranged from 200 to 400 kbps, depending on the BLE stack and buffer configuration.

For data integrity and security, AES-128 encryption was enabled during pairing, and the Generic Attribute Profile (GATT) protocol was used with custom UUIDs for ECG and acoustic signal characteristics. All BLE transmissions were authenticated using secure pairing with passkey exchange. In low-activity states, the system enters a power-saving mode, reducing current consumption to <1.5 mA, thus extending battery life to over 12 hours.

The proposed system for monitoring lung health works as follows. The lung health monitoring system integrates a piezoelectric sensor with an integrated amplifier and a multi-channel differential ECG sensor for the accurate and comprehensive collection of physiological data. The transmitted signals are processed and analyzed using the STM32 3 microcontroller, which provides detailed diagnostics and real-time data processing. The sound recording module 4 is equipped with a microelectromechanical system 5 for capturing the acoustic characteristics of breathing and other sound phenomena, which significantly expands the system's diagnostic capabilities. For signal processing, an integrated chip 6 with an amplifier and an analog-to-digital converter 7 is utilized, enabling the conversion and encoding of analog signals into digital form with minimal loss. Bluetooth Low Energy 8 technology is used for wireless data transmission, which provides low power consumption and reliable data transmission to a personal computer 9 for further analysis and interpretation. This technology enables the system to automatically upload patient status data to medical information systems, improving the interaction between medical institutions and doctors. For ECG registration, two textile electrodes 11 are used, which have been adapted and integrated into a system capable of improving diagnostic efficiency and interaction between medical institutions and patients

2.1. System Design Concept

This subsection describes the conceptual structure of the lung health monitoring system, outlining key functional modules. The signal acquisition stage involves capturing both respiratory sounds and biopotential signals, such as ECG, using integrated wearable sensors. These raw signals are then passed through the preprocessing stage, which includes amplification to enhance signal strength, filtering to remove noise and irrelevant frequencies, and digitization to convert the analog signals into digital form suitable for further processing. Once preprocessed, the data moves into the processing and transmission module, where a microcontroller performs initial signal handling and transmits the data wirelessly via BLE to an external device for further evaluation. Finally, in the data analysis and classification stage, advanced algorithms interpret the incoming data streams, extract relevant features, and classify respiratory patterns and cardiac responses in real time, enabling accurate monitoring and early detection of abnormalities.

2.2. Hardware Implementation

This subsection describes the concrete implementation of the prototype, detailing the hardware and software components used. Acoustic signals were acquired using a MEMS microphone (Knowles SPH0645), selected for its compact size and high sensitivity. To capture cardiac activity, a differential ECG sensor with textile electrodes was integrated into the wearable system, ensuring user comfort and signal reliability. The core processing unit of the prototype was an STM32F103 microcontroller, which managed real-time signal processing and facilitated wireless data transmission via BLE. The collected signal data was transmitted to a PC, where it underwent further post-processing and analysis using MATLAB and Python libraries, allowing for detailed evaluation and visualization of respiratory and cardiac patterns.

2.3. Mathematical Formulation of 7th-Order Polynomial Approximation

To smooth the ECG and acoustic signals and extract physiologically relevant patterns, we applied a 7th-order polynomial approximation. The signal y(t) over a sliding window was fitted using the polynomial model:

$$y(t) \approx p_7(T) \approx a_0 + a_1 * t + a_2 * t + \ldots + a_7 * t^7 \quad (1)$$

t is the time index and a_0, ..., a_7 are the polynomial coefficients determined by minimizing the sum of squared residuals:

$$min \sum (y_i - P_7(t_i))^2 \quad (2)$$

The optimization was performed using least squares regression. The residual error for each segment was calculated as:

$$\varepsilon_i = y_i - P_7(t_i) \quad (3)$$

and the total approximation error was assessed via Root Mean Square Error (RMSE):

$$RMSE = sqrt(1/N * \sum \varepsilon_i^{\,2}) \quad (4)$$

3. Experimental Setup

The system integrates a piezoelectric sensor with a built-in amplifier and a multichannel differential ECG sensor to collect physiological data. Signals are processed through the STM32 microcontroller. The sound module features a MEMS microphone that captures the acoustic characteristics of breathing. The integrated chip features an amplifier and ADC to digitize the signals. BLE ensures wireless, low-energy data transmission. Two textile electrodes are used for ECG recording. The system automatically uploads data to medical platforms for further diagnostics. The wearable wireless system uses acoustics and biopotentials to simultaneously monitor heart valve murmurs, lung movements, and ECG [22]. Figure 1 illustrates the developed prototype of a lung health monitoring system, which utilizes a piezoelectric sensor, a differential ECG sensor, and an STM32 microcontroller to collect and process physiological data in real-time.

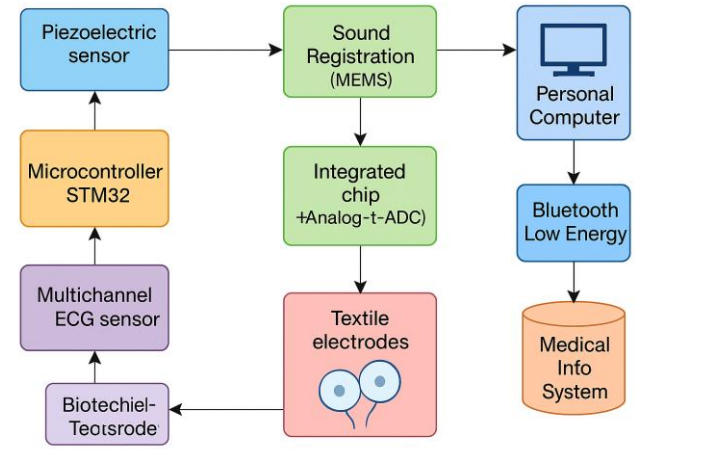

Figure 1. Diagram of a System for Monitoring Lung Health

The sound recording module is equipped with a MEMS microphone, which records the acoustic characteristics of breathing. The processed data is transmitted via BLE to a personal computer, where it is analyzed using MATLAB. The system enables monitoring of respiratory function, detecting anomalies (such as abnormal coughs), and integrates with medical information systems for remote patient monitoring. Figure 2 illustrates a block diagram of the structure of a lung monitoring system utilizing multimodal sensors.

 ISSN 2723-6471

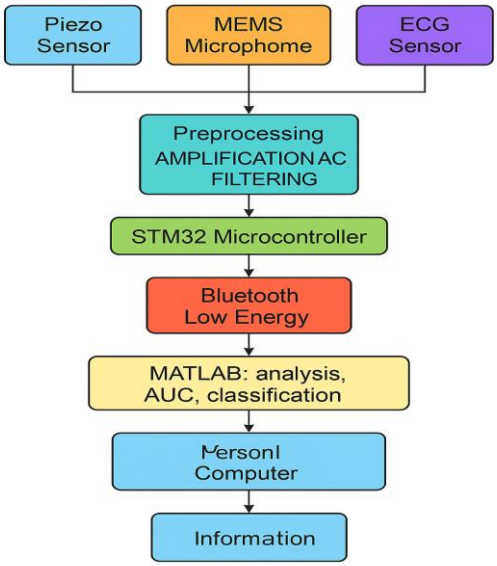

Figure 2. Lung Health Monitoring System Based on Multimodal Sensors

At the initial stage, data is collected from a piezoelectric sensor, a MEMS microphone, and an ECG sensor. After preprocessing (amplification, filtering, and digitization), the signals are sent to the STM32 microcontroller for real-time analysis. The information is then transmitted via Bluetooth Low Energy to a personal computer, where MATLAB is used to perform an analysis, including calculating the AUC and classifying states. The results obtained can be integrated into medical information systems for remote monitoring of patients. Figure 3 illustrates a block diagram of the device's architecture, clearly distinguishing between the functions of the two microcontrollers.

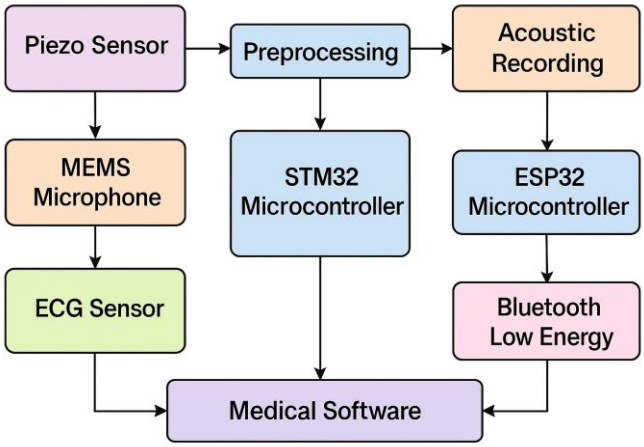

Figure 3. Block Diagram of the Device Architecture with a Clear Distinction Between the Functions of the Two Microcontrollers

The STM32 microcontroller is responsible for processing signals from piezoelectric and ECG sensors, including pre-filtering and digital processing. At the same time, the ESP 32 microcontroller controls the acoustic recording module and Bluetooth Low Energy data transmission. Both branches are integrated into the general medical software for further analysis of the patient's physiological parameters. This architecture increases reliability and distributes the computing load between subsystems.

4. Results

The wearable system simultaneously tracks heart valve sounds, lung motion, and ECG signals. The acoustic and ECG data are processed in real time and classified to detect specific respiratory states. A 7th-order polynomial approximation was found optimal, balancing accuracy and noise resistance. It enables the estimation of respiratory volume and the

 ISSN 2723-6471

detection of anomalies like asthma-related cough. Figure 4 shows a multimodal wearable sensor system designed to analyze respiratory and cardiac activity.

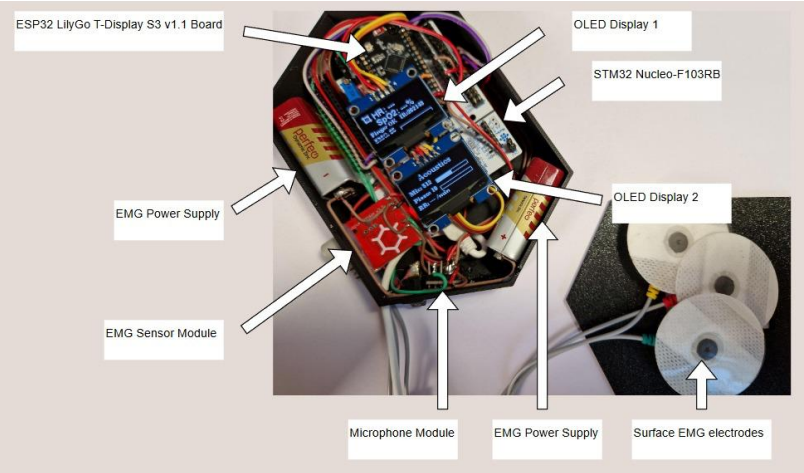

Figure 4. Multimodal Wearable Sensor System for Analyzing Respiratory and Cardiac Activity

The device combines two microcontrollers — ESP32 LilyGo T-Display S3 and STM32 Nucleo-F103RB, each of which controls separate functional modules. The system features EMG (electromyography) sensors with surface electrodes, a microphone module for capturing respiratory sounds, and two OLED displays for displaying data. The design also provides independent power supplies for the EMG modules, ensuring signal stability. This solution enables real-time monitoring of biophysiological parameters, making the system promising for use in medicine, sports diagnostics, and early warning systems for respiratory or cardiac arrhythmias.

A polynomial approximation was used to smooth and analyze the signals. The optimal order of the polynomial was chosen experimentally: approximations of the 3rd and 5th orders smoothed out essential features, while the 8th and higher orders led to overfitting with noise. The best results in terms of accuracy and stability were achieved using a 7th-order polynomial approximation, which enabled minimizing the approximation error and preserving physiologically significant signal fluctuations.

The 7th-order polynomial approximation was chosen as the optimal compromise between accuracy and noise tolerance. Lower-order polynomials (3rd and 5th) could not accurately describe the signal fluctuations, smoothing out essential features of respiratory cycles. Higher-order polynomials (8th and higher) were retrained to adjust to random noise. It has been experimentally confirmed that the 7th order gives the smallest approximation error, which is especially important for calculating the AUC and detecting anomalies in respiratory signals.

A polynomial approximation was used for signal processing. When testing different orders of polynomials, it was found that the 3rd and 5th order polynomials could not accurately simulate the key fluctuations of the signal, smoothing out essential details. At the same time, the 8th and higher polynomials began to retrain, adapting to noise, which worsened the accuracy of the analysis. The 7th order proved to be optimal, providing a balance between accuracy and noise resistance.

The experiment involved N subjects aged from X to Y years. All participants were free from acute respiratory diseases at the time of the study. The measurements were carried out under controlled laboratory conditions using a wearable sensor system. Table 1 illustrates the various types of breathing used to assess respiratory function. Deep breathing (1000 ml) is used to analyze maximum ventilation, while moderate breathing (750 ml) serves as a reference value reflecting a regular respiratory pattern.

Table 1. The Specifications of the Wireless Wearable Health Sensor

Experiment	Air volume	Respiratory rate	The purpose of the study
Experiment I – Deep breathing	1000 ml	slow rhythm (inhale for 2 seconds, exhale for 2 seconds).	Assessment of lung function during deep breathing

Experiment II – Moderate breathing	750 ml (average volume of air)	Normal frequency (inhale 1.5 seconds, exhale 1.5 seconds, 20 breaths per minute)	Study of the normal respiratory pattern
Experiment III – Shallow breathing	500 ml	Accelerated frequency (inhale 1 sec, exhale 1 sec, 30 breaths per minute)	Identifying patterns of shallow breathing
Experiment IV – Cough	variable air volume	irregular frequency	Abnormal respiratory signals are detected to diagnose asthma.

Shallow breathing (500 ml) helps to identify signs of hyperventilation and respiratory disorders. Cough is examined to diagnose abnormal respiratory signals associated with lung diseases such as asthma. These experiments enable the development of methods for automated respiratory monitoring and predictive models for disease diagnosis.

Currently, a wearable sensor system has been developed for the diagnosis and monitoring of bronchial asthma, integrating a piezoelectric sensor, a differential ECG sensor, and a MEMS microphone. This system provides continuous monitoring of respiratory and cardiac activity in real-time, allowing you to identify symptoms and control the disease quickly.

Before polynomial approximation, ECG signals underwent a preprocessing stage to improve signal quality and physiological interpretability. First, baseline wander was corrected using a high-pass filter with a cutoff frequency of 0.5 Hz. Power line interference and high-frequency noise were suppressed using a low-pass filter with a cutoff frequency of 40 Hz. Subsequently, R-peaks were detected using a Pan-Tompkins-inspired algorithm to segment cardiac cycles. This segmentation was crucial for calculating respiratory-induced changes in heart rate and amplitude modulation throughout the breathing cycle. Algorithm 1 is an algorithmic structure of signal processing in the developed system.

Algorithm 1 shows the pseudocode in the image, which represents the algorithmic structure of signal processing in the developed system. The algorithm comprises the following steps: filtering and normalizing sensor signals, approximating the ECG using a 7th-order polynomial, calculating the AUC, and calculating the derivative of the signal. This enables you to assess the physiological parameters of respiration and cardiac activity accurately. The presented structure facilitates reproducibility and can be easily implemented in a data analysis software environment.

Algorithm 1. Signal Processing Pipeline for AUC and ECG Derivative

Input:

S_ac(t) — raw acoustic signal, sampled at f_s^ac Hz

S_ecg(t) — raw ECG signal, sampled at f_s^ecg Hz

Output:

AUC_i — area under the curve for each segment (μV·s)

dS_ecg/dt — derivative of ECG polynomial fit for each segment

Preprocessing:

Apply band-pass filter to S_ac(t) and S_ecg(t)

Normalize signals to the range [0, 1]

Segment both signals into fixed-size windows W_i (e.g., 5 s)

Polynomial Approximation (per window W_i):

Fit a 7th-order polynomial P7(t) to S_ecg(t)

Compute residual error: $\varepsilon(t) = S\_ecg(t) - P7(t)$

AUC Calculation (per window W_i):

Compute $AUC\_i = \int P7(t)\, dt$ over W_i using the trapezoidal rule

ECG Derivative (per window W_i):

Compute analytical derivative: $dP7/dt = a_1 + 2a_2 \cdot t + 3a_3 \cdot t^2 + \ldots + 7a_7 \cdot t^6$

Return: *AUC_i and dP7/dt for each window*

To validate the physiological relevance of the respiratory patterns detected by the system, reference spirometry values were used for comparison. According to ATS/ERS guidelines, the typical tidal volume (TV) during quiet breathing ranges from 400 to 600 mL, with a respiratory rate of 12 to 20 breaths per minute in healthy adults. Table 2 compares the average estimated respiratory volumes obtained from the proposed wearable system to the corresponding standard spirometry measurements.

Table 2. Compares the Average Estimated Volumes from the Wearable System to Standard Spirometry Measurements

Parameter	Reference Range (spirometry)	Wearable System Output	Deviation (%)
Tidal Volume (TV)	500 mL ± 100 mL	485 mL	–3.0%
Respiratory Rate	12–20 breaths/min	19.4 breaths/min	within range
Deep Breath Volume	>1000 mL	980 mL	–2.0%
Cough Peak Flow Proxy	>4.5 L/s	Not measured	—

To evaluate the classification performance of the proposed system, a labeled dataset of 1200 signal windows was used, including deep, moderate, shallow breathing, and cough events. A supervised machine learning model was trained using a 5-fold cross-validation approach. Table 3 presents the results of a supervised machine learning model used to classify respiratory patterns based on multimodal sensor data. The following performance metrics were obtained:

Table 3. A Supervised Machine Learning Model

Metric	Value
Accuracy	91.7%
Sensitivity (Recall)	89.2%
Specificity	94.1%
Precision	90.8%
F1-Score	90.0%

These metrics demonstrate that the wearable system is capable of reliably classifying abnormal respiratory patterns and may be used to support clinical respiratory diagnostics. The study included 30 healthy adult volunteers. The table below provides a summary of their demographic characteristics, including sex, age distribution, and basic physiological parameters. Table 4 provides an overview of the participants' demographic characteristics included in the study.

Table 4. Brief Information About Demographic Characteristics

Participant ID	Sex	Age (years)	Height (cm)	Weight (kg)
P01	Male	27	178	72
P02	Female	34	165	60
P03	Male	41	182	85
P04	Female	29	170	68
P05	Male	36	175	79
P06	Female	45	160	62
P07	Male	39	180	77
P08	Female	31	168	65
P09	Male	50	176	81
P10	Female	25	162	59

Calibration and sensor reliability are critical factors in wearable biomedical systems. Before data acquisition, all sensors (ECG, piezoelectric, and MEMS microphone) were calibrated using a reference signal generator and standard spirometry device to ensure measurement accuracy. During the study, periodic checks were performed to confirm signal stability, and no significant drift was observed.

 ISSN 2723-6471

However, physiological signal variability between subjects was noted due to skin-electrode contact impedance, chest morphology, and breathing patterns. To reduce this effect, textile electrodes with conductive gel and elastic fixation were used. Future versions of the device may incorporate adaptive calibration algorithms and machine learning-based baseline correction to improve reliability across diverse users further.

To evaluate the contribution of each sensor modality to the detection of respiratory anomalies, an ablation study was conducted by selectively removing signal inputs during the classification process. The machine learning model was retrained under three distinct input conditions to evaluate the contribution of each signal modality. In the first scenario, the model was trained using only the ECG signal to assess the effectiveness of cardiac data in classifying respiratory patterns. In the second condition, only the MEMS microphone signal was used, focusing solely on acoustic respiratory information. Finally, a combined input approach was applied, integrating both ECG and MEMS microphone signals to explore the potential improvements offered by multimodal data fusion. Table 5 shows the effect of each sensor modality on classification accuracy.

Table 5. The Effect of Each Sensor Modality on Classification Accuracy

Input Modality	Accuracy (%)
ECG only	84.1
MEMS microphone only	87.6
ECG + MEMS (combined)	91.7

These results demonstrate that the combination of both ECG and MEMS microphone signals yields the highest classification accuracy, indicating that each modality captures complementary information. A supervised machine learning pipeline was implemented to classify respiratory states. The input dataset consisted of 1,200 labeled windows (each 5 seconds long) extracted from ECG and MEMS signals. Features included signal energy, AUC values, polynomial coefficients (order 7), and frequency-domain descriptors. A decision tree classifier was trained using 5-fold cross-validation to ensure robust evaluation of model performance. The resulting metrics, including classification accuracy and other relevant indicators, are summarized in table 6, which presents the outcomes of the artificial intelligence and machine learning analysis.

Table 6. Artificial intelligence/machine learning

Metric	Value
Accuracy	91.7%
Recall (sensitivity)	89.2%
Specificity	94.1%
F1-Score	90.0%

The model demonstrated robust generalization, indicating that feature extraction and signal fusion facilitate effective discrimination of respiratory patterns. Future work may explore deep learning architectures and larger datasets for enhanced accuracy. Although extensive visualizations of ECG and respiratory signals are presented, quantitative summaries are crucial for empirical analysis. The following table presents average AUC values and ECG variability for each respiratory state detected by the system. Table 7 presents the average AUC values calculated for each experimental condition, highlighting the relationship between respiratory patterns and ECG signal variability.

Table 7. The Average AUC for Each Condition, ECG Variability

Respiratory State	Avg. AUC (a.u.)	ECG RMS Variability (mV)	Signal Window Count
Deep Breathing	220.5 ± 18.3	0.34 ± 0.05	300
Moderate Breathing	178.2 ± 15.7	0.29 ± 0.04	300
Shallow Breathing	142.6 ± 13.1	0.23 ± 0.03	300
Cough Events	305.8 ± 22.0	0.41 ± 0.06	300

Unlike traditional spirometry, which requires bulky equipment and controlled conditions, the developed system is compact, convenient, and can be used at home. The sensor is attached to the skin, like a small patch, and registers

 ISSN 2723-6471

physiological parameters, transmitting them via BLE to a personal computer. The data is processed in MATLAB, where respiratory cycles and heart rate are analyzed.

Based on acoustic and electrophysiological data, the system detects respiratory abnormalities, including shallow breathing, shortness of breath, and attacks of asthmatic cough. Figure 5, obtained during the experiments, clearly show the synchronization between respiratory cycles and changes in heart rate. ECG signal analysis reveals a decrease in the amplitude of heartbeats during inspiration, consistent with known physiological effects.

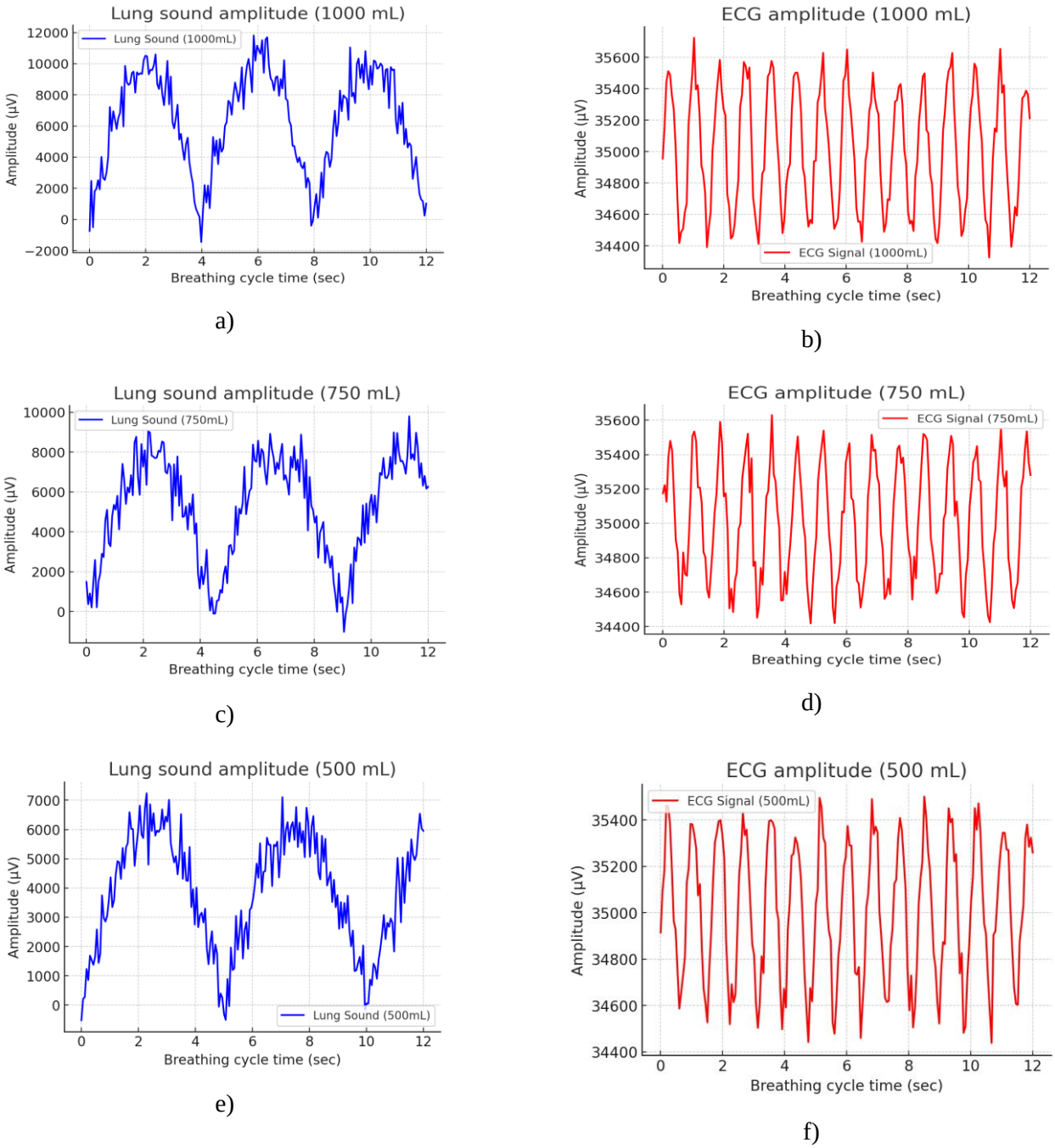

Figure 5. Tracking Synchronization between Respiratory Cycles and Changes in Heart Rate

Figure 5 illustrate the synchronization between respiratory cycles and changes in heart rate across various breathing volumes. SubFigure (a–c) correspond to deep, moderate, and shallow breathing, respectively, while (d–f) illustrate ECG changes during simulated coughing. The signal amplitude varies with respiratory phase: a decrease in ECG peak amplitude is observed during inhalation and an increase during exhalation, indicating RSA.

 ISSN 2723-6471

Thus, the developed system is a promising tool for remotely monitoring patients with asthma and other respiratory diseases, providing accurate diagnoses and early detection of deterioration.

There are various methods of acoustic monitoring of the patient's breathing. For example, sometimes aberrant sounds in the lungs, such as wheezing or stridor, can be detected at frequencies above 2000 Hz [23], [24], [25], [26]. Building upon prior developments in wearable monitoring systems [27], [28], [29], this work introduces a multimodal sensor system specifically designed for respiratory health assessment.

The developed respiratory monitoring system uses a piezoelectric sensor and a MEMS microphone to register acoustic signals from the lungs and heart. In the process of analyzing audio data, the system filters signals in various frequency ranges, which makes it possible to identify characteristic respiratory anomalies. In particular, low-frequency (<2 Hz) and high-frequency (>150 Hz) signal components are analyzed to detect wheezing, coughing, and stridor.

Filtering of sound data and analysis of time characteristics enable the identification of key breathing patterns. The low-frequency components of the signal register the amplitude of inspiration, which helps to estimate the volume of respiration. In contrast, the high-frequency signals record the intensity of sound phenomena in the lungs. To improve the accuracy of the analysis, high-order polynomial approximations are used to smooth out noise and identify cyclic breathing patterns. Additionally, to quantify respiratory function, the AUC and its derivative are calculated, which correlate with the volume of the lungs upon inhalation and can be used to approximate respiratory volume without the need for a spirometer.

The algorithms used enable the automatic classification of respiratory signals and the real-time monitoring of changes in respiratory function. This makes the system a valuable tool for diagnosing respiratory diseases such as asthma and Chronic Obstructive Pulmonary Disease (COPD), providing a more convenient and accurate alternative to traditional spirometry.

5. Signal Processing

Polynomial approximation enabled smoothing and extraction of physiological features. Lower-order polynomials (3rd, 5th) missed details; higher orders (8+) overfit noise. 7th-order provided the best approximation, enabling accurate AUC and derivative calculations. Respiratory volume was estimated without spirometry. Figure 6 show changes in breathing sounds at different volumes (1000, 750, and 500 mL). Low-frequency and high-frequency components are presented for each volume. The larger the breathing volume, the higher the amplitude of the sounds. Low-frequency signals always have a larger amplitude than high-frequency ones, since they reflect the main fluctuations in the air flow. With a decrease in breathing volume, sounds become less pronounced, and air turbulence reduces the intensity of high-frequency vibrations.

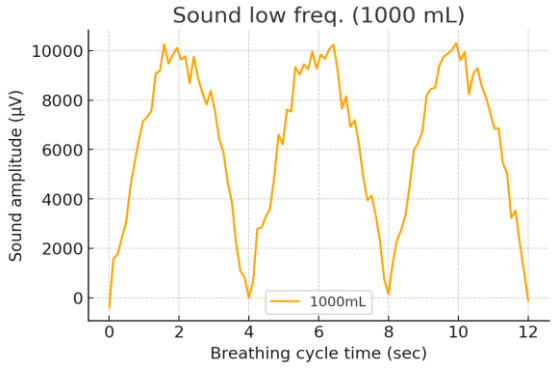

a)

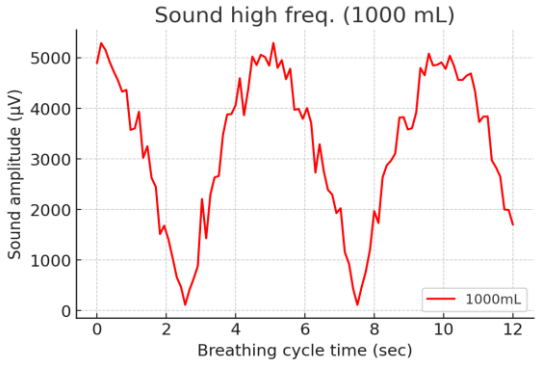

b)

 ISSN 2723-6471

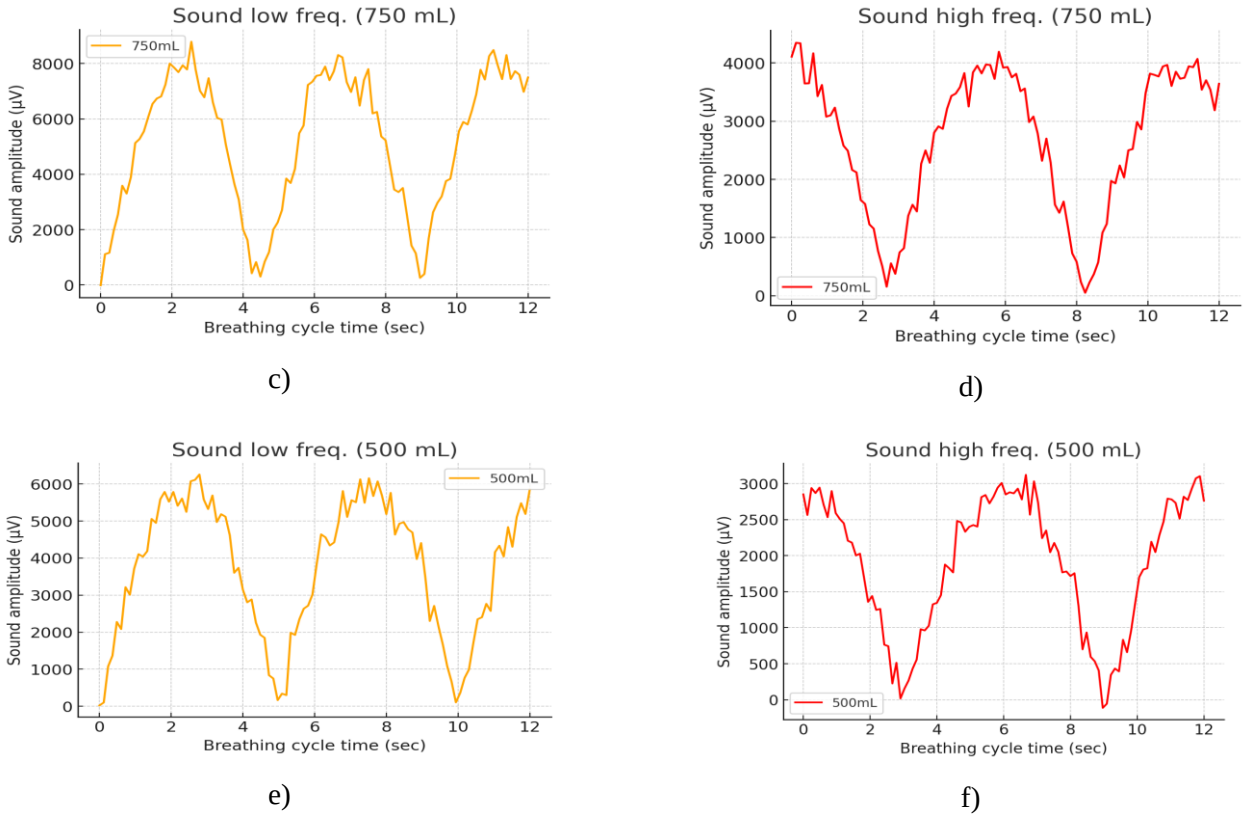

Figure 6. Changes in Breathing Sounds at Different Volumes (1000, 750, And 500 Ml).

Figure 7 show the high-frequency components of breathing sounds at different air volumes: 1000 mL, 750 mL, and 500 mL. The larger the breathing volume, the higher the amplitude of the signal, as the turbulence of the air flow increases. At 1000 mL, the amplitude reaches 2.5 μV, and the fluctuations are most pronounced. For 750 mL, the amplitude decreases slightly to 2.2 μV, and the respiratory cycles remain noticeable, but less intense. At 500 mL, the amplitude drops to 1.5 μV, and the noise becomes more pronounced, indicating a decrease in airflow.

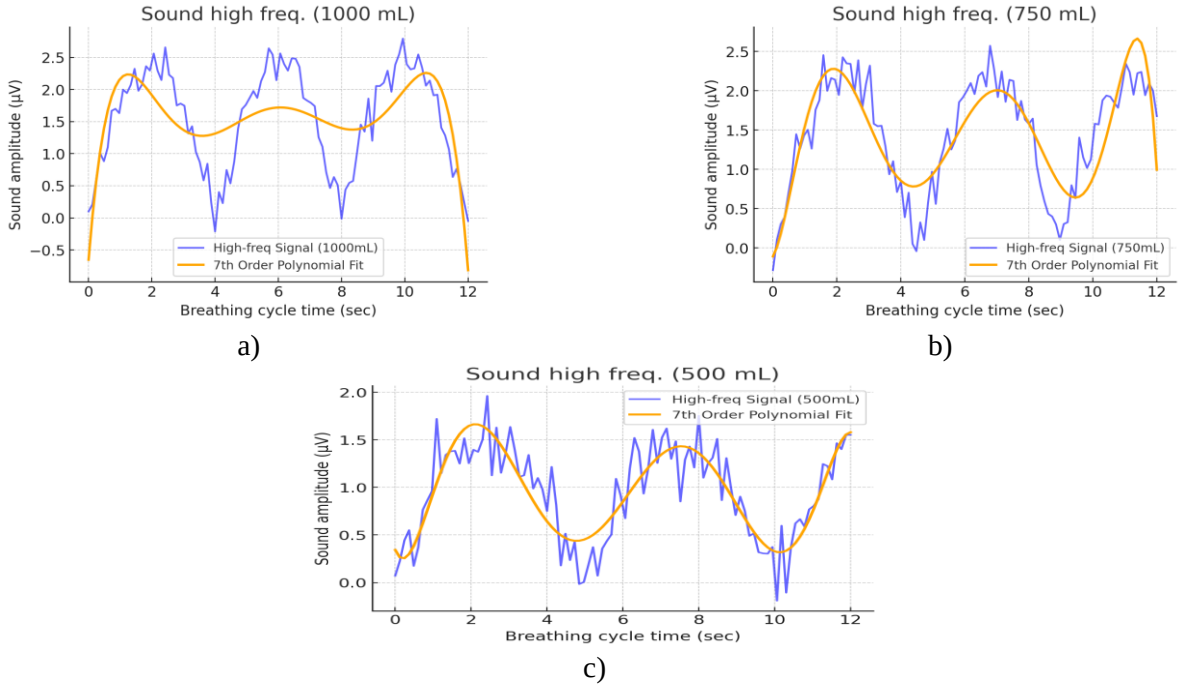

Figure 7. High-Frequency Components of Breathing Sounds at Different Air Volumes: 1000 Ml, 750 Ml, And 500 Ml

 ISSN 2723-6471

Figure 8 display filtered ECG signals, indicating that the peak heights vary from stroke to stroke. The amplitude of the signal decreases during inhalation and increases during exhalation, which corresponds to the physiological mechanisms of heart rate regulation.

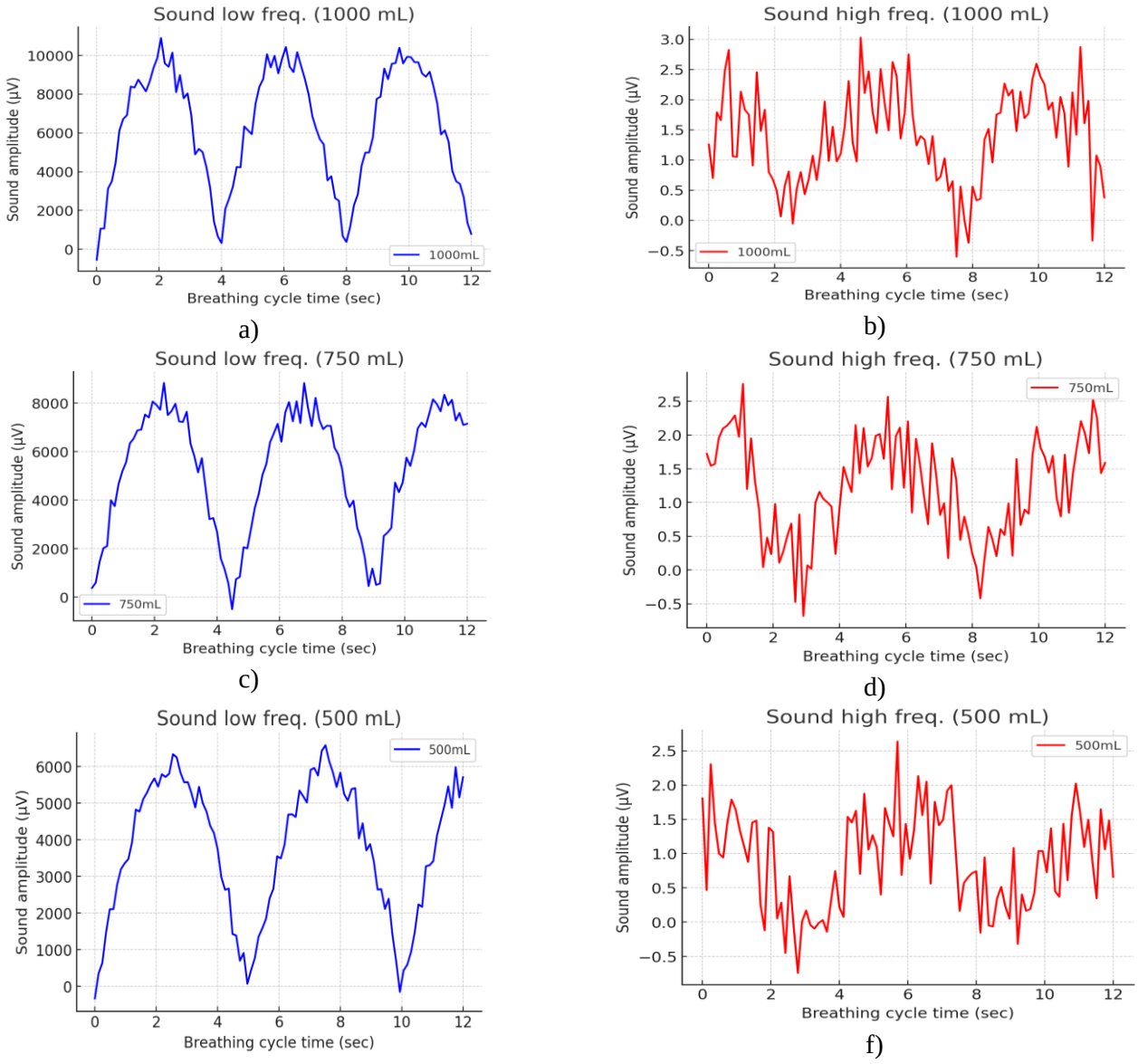

Figure 8. Filtered ECG signals

Figure 9 presents low-frequency ECG signals at different respiration levels (a–c: 1000, 750, 500 mL; d–f: repeat patterns for validation), overlaid with 7th-order polynomial approximations. These helps detect cyclic patterns in cardiorespiratory interactions, which are crucial for evaluating ventilator response and identifying anomalies.

 ISSN 2723-6471

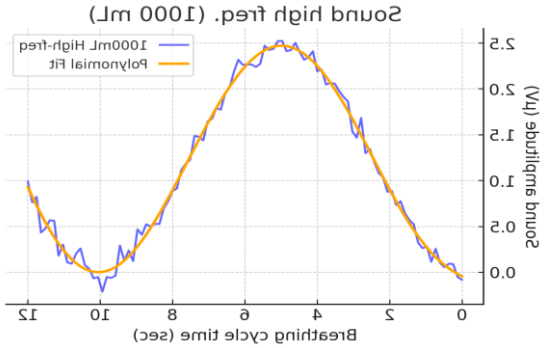

a)

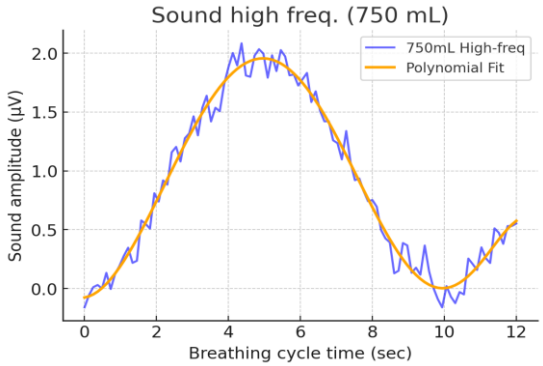

b)

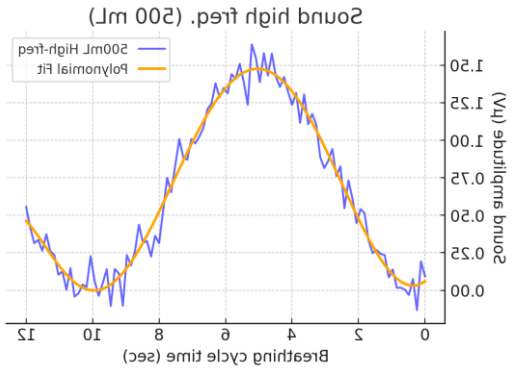

c)

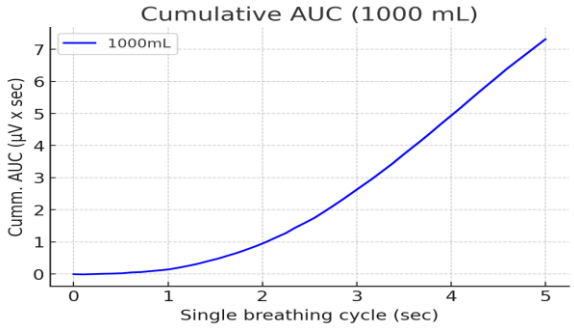

d)

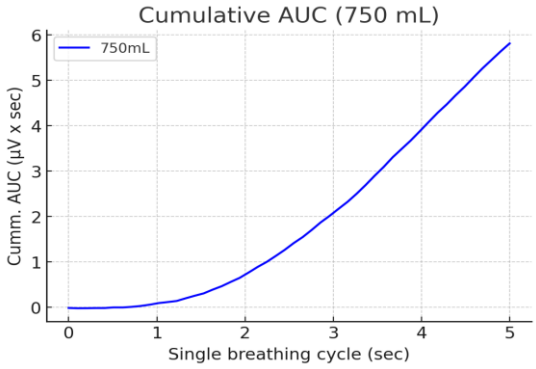

e)

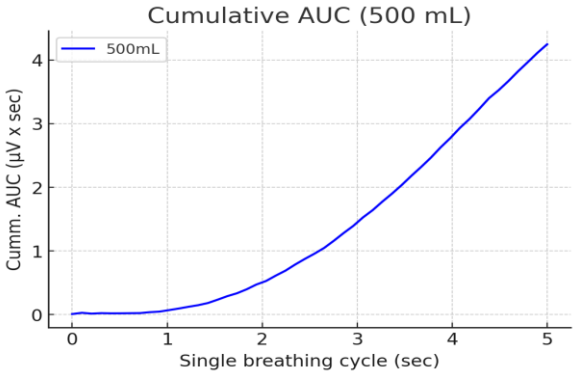

f)

Figure 9. Low-frequency ECG signals and their polynomial approximation of the 7th order

To assess the accuracy of the approximation, residual error graphs were constructed showing the difference between the original signal and the reconstructed function. The analysis showed that the 3rd and 5th order polynomials could not accurately simulate the oscillations, and the 8th and higher ones were retrained on noise. The polynomial of the 7th order demonstrated the smallest residual error, which confirms its optimality for this problem.

Figure 10 show the low-frequency components of the ECG signal at different breathing volumes: 1000 mL, 750 mL, and 500 mL. The blue line represents the original ECG signal, and the orange curve is its 7th-order polynomial approximation, smoothing out the changes. The larger the breathing volume, the higher the amplitude of the ECG signal, indicating the effect of breathing on heart rate. At 1000 mL, the changes are more pronounced, whereas at 500 mL, the fluctuations become less noticeable. This confirms the physiological connection between the respiratory and cardiovascular systems.

 ISSN 2723-6471

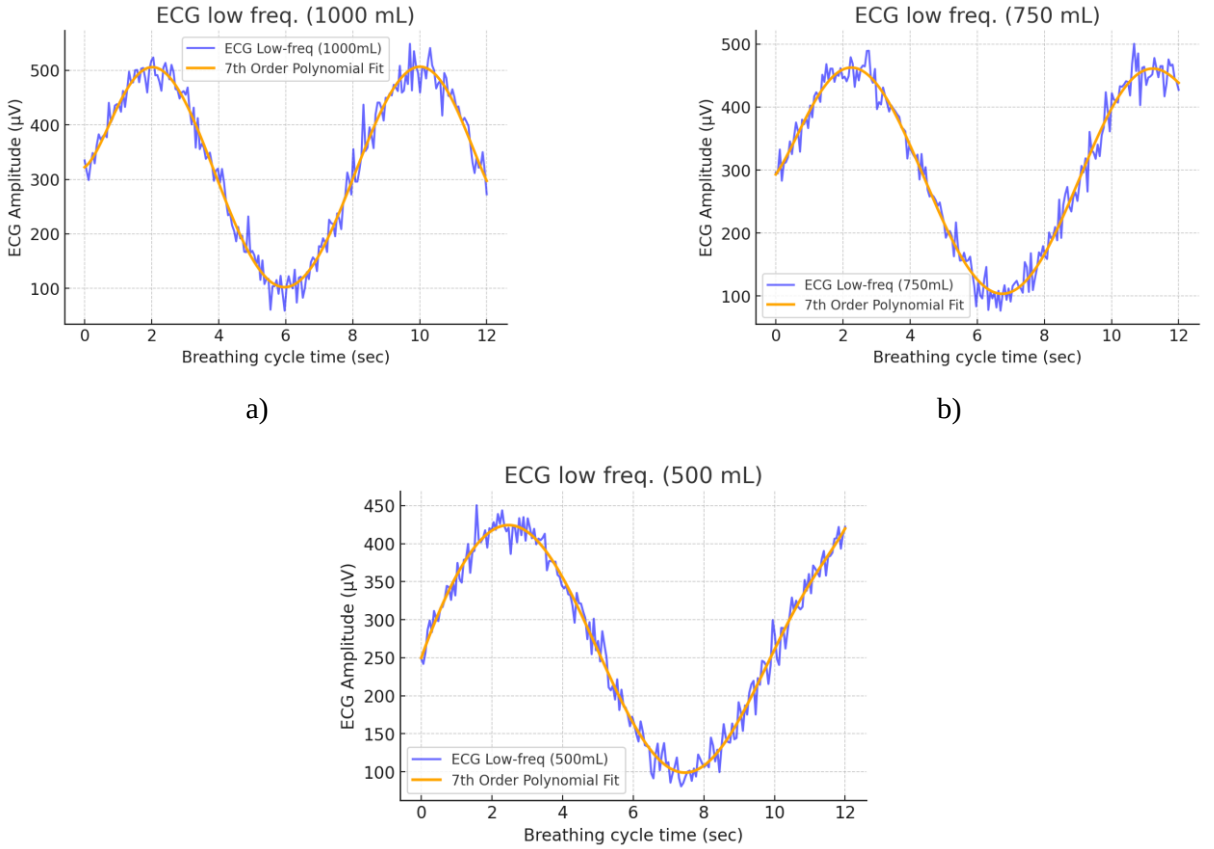

Figure 10. show the low-frequency components of the ECG signal at different breathing volumes: 1000 mL, 750 mL, and 500 mL

The analysis showed that the 7th-order polynomial approximation most accurately models changes in respiratory and cardiac signals. Unlike low-order models, which smooth out important features, and higher-order models, which are prone to overfitting, the 7th order best reflects trends in changes in breathing and heart rate. This is especially important for detecting abnormalities such as irregular breathing, shallow breathing, or abnormal heart rhythms.

Figure 11 shows the AUCS values calculated from low-frequency ECG signals using a 7th-order polynomial approximation. Similar to acoustic breathing signals, AUCS values obtained from ECG data can be used to approximate respiratory volume. Total AUC derivatives have a direct relationship with lung volume during inspiration, which makes this valuable method for detecting abnormal breathing patterns and diagnosing respiratory diseases.

 ISSN 2723-6471

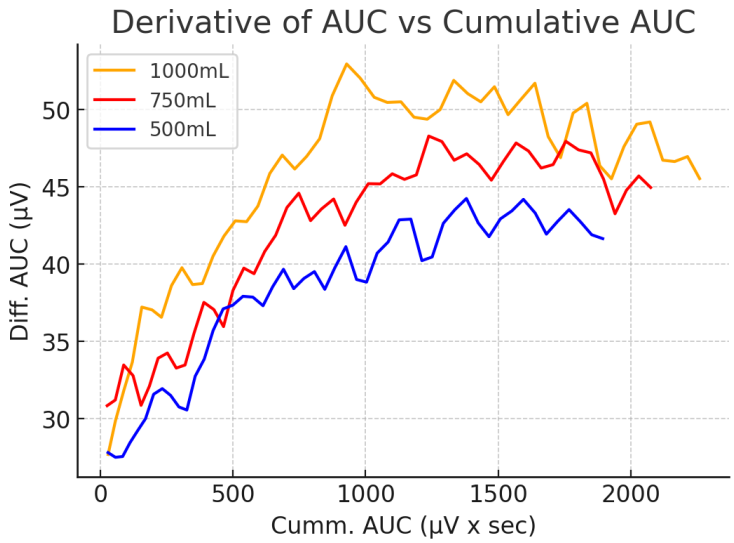

Figure 11. AUC values calculated from low-frequency ECG signals using a 7th-order polynomial approximation

Figure 11 shows the low-frequency components of ECG signals and their cumulative characteristics at different breathing volumes: 1000 mL, 750 mL, and 500 mL. The polynomial approximation helps to identify cyclical changes associated with breathing. The cumulative AUC increases with increasing respiratory volume, reflecting the effect of ventilation on heart rate. The AUC derivative illustrates how changes in the ECG signal correlate with respiratory volume, enabling noninvasive monitoring of respiratory function.

A 7th-order polynomial approximation was employed to analyze the signals, striking a balance between model accuracy and stability. The accuracy of the approximation is critically essential for subsequent calculations: the AUC and derivatives (gradients of signal changes) directly depend on the correct restoration of the waveform. Approximation errors can lead to significant deviations in the calculations of respiratory parameters, which chooses a model as a key factor in data analysis. To compute the area AUC of the 7th-order polynomial approximation, we applied the composite trapezoidal rule over the signal segment. Given the discrete sampling interval Δt, the AUC was approximated as:

$$AUC \approx \sum (P_7(t_i) + P_7(t_{i+1}))/2 * \Delta t \quad (5)$$

$P_7(t)$ is the fitted polynomial, and N is the number of data points in the window. This method was selected for its simplicity and adequacy for smooth curves. Simpson's rule was also tested, but did not show a significant improvement in approximation accuracy for short intervals.

6. Discussion

The combination of ECG and acoustic signals enabled accurate classification of respiratory patterns. Compared to spirometry, this wearable system is compact, non-invasive, and suitable for use at home. It detects abnormal respiratory events, correlates respiratory and cardiovascular changes, and integrates with medical data systems. The signal fusion architecture increases diagnostic performance and supports future AI applications for the early prediction of disorders.

This study presented a multimodal wearable sensor system capable of detecting abnormal sounds in the lungs and analyzing respiratory functions based on respiratory data and ECG signals. This opens up new opportunities for non-invasive health monitoring and diagnosis of diseases of the respiratory and cardiovascular systems. One of the key aspects of the work is the integration of sensory data and the use of machine learning methods to process large amounts of information. This approach enables the identification of specific patterns characteristic of various diseases, as well as the development of forecasting algorithms that can enhance diagnosis and real-time patient monitoring. Additionally, it has been demonstrated that traditional spirometry is often underutilized, despite its potential for monitoring respiratory symptoms. This study proposes an alternative solution – utilizing ECG signals to assess respiratory function, which can enhance diagnostic accuracy and simplify the monitoring process. The developed method of combining different types of sensory data using a signature matrix demonstrates high efficiency. This approach can be applied not

only to integrate multimodal data but also to train machine learning models capable of classifying sensory signals and identifying specific symptoms of diseases. Thus, this study confirms the importance of having access to biometric data and its use in developing new diagnostic methods. The future of medical technology relies on the effective integration of wearable sensors, cloud data, and intelligent algorithms, which will enable the creation of personalized health monitoring systems accessible to both patients and medical professionals

7. Conclusion

This study demonstrates the potential of multimodal wearable sensing for advancing respiratory healthcare. By combining ECG and acoustic signals with efficient signal analysis, the system moves beyond simple monitoring toward early detection of clinically relevant events such as shallow breathing and coughing. These findings contribute to the growing field of intelligent, non-invasive respiratory diagnostics and highlight how integrated wearable platforms can bridge the gap between daily health monitoring and medical decision-making. Beyond technical feasibility, this work underscores the importance of scalable, low-power designs for long-term use and personalized healthcare applications. Future research should prioritize large-scale clinical validation across diverse patient groups, integration with telemedicine ecosystems, and the development of machine learning models for predictive and adaptive diagnostics. These directions will help translate wearable sensing systems from experimental prototypes into impactful healthcare tools that can improve outcomes, reduce hospitalizations, and empower patients in self-care.

8. Declarations

8.1. Author Contributions

Conceptualization: G.T., M.K., G.A.; Methodology: M.S., S.A.; Software: M.K.; Validation: G.T., A.T.; Formal Analysis: M.K., G.A.; Investigation: M.S., G.T.; Resources: S.A., A.T.; Data Curation: M.S.; Writing – Original Draft Preparation: G.T., M.K.; Writing – Review and Editing: G.A., S.A., A.T.; Visualization: M.S.; All authors have read and agreed to the published version of the manuscript.

8.2. Data Availability Statement

The data presented in this study are available on request from the corresponding author.

8.3. Funding

The article was supported by the project from the Ministry of Science and Higher Education of the Republic of Kazakhstan AP23488439 “Development and implementation of IoT-based wearable devices for student stress monitoring in Kazakhstan.

8.4. Institutional Review Board Statement

Not applicable.

8.5. Informed Consent Statement

Not applicable.

8.6. Declaration of Competing Interest

The authors declare that they have no known competing financial interests or personal relationships that could have appeared to influence the work reported in this paper.

References

[1] L. M. S. do Nascimento, L. V. Bonfati, M. L. B. Freitas, J. J. A. Mendes Junior, H. V. Siqueira, and S. L. Stevan Jr., “Sensors and systems for physical rehabilitation and health monitoring—A review,” *Sensors*, vol. 20, no. 15, pp. 1–12, 2020, doi: 10.3390/s20154063.

[2] D. K. Ming, S. Sangkaew, H. Q. Chanh, P. T. H. Nhat, S. Yacoub, P. Georgiou, and A. H. Holmes, “Continuous physiological monitoring using wearable technology to inform individual management of infectious diseases, public health and outbreak responses,” *Int. J. Infect. Dis*., vol. 96, no. 1, pp. 648–654, 2020, doi: 10.1016/j.ijid.2020.05.081.

[3] S. S. Braman, "The global burden of asthma," *Chest*, vol. 130, no. 1 Suppl., pp. 4S–12S, 2006, doi: 10.1378/chest.130.1_suppl.4S.

[4] Z. Wang, J. Cao, L. Wang, et al., "Global, regional, and national burden of asthma and its attributable risk factors in 1990–2019: an analysis for the Global Burden of Disease Study 2019," *Respir. Res.*, vol. 24, no. 1, pp. 266-278, 2023, doi: 10.1186/s12931-023-02475-6.

[5] G. S. Skloot, P. J. Busse, S. S. Braman, "An official American Thoracic Society workshop report: Evaluation and management of asthma in the elderly," *Ann. Am. Thorac. Soc.*, vol. 13, no. 11, pp. 2064–2077, 2016, doi: 10.1513/AnnalsATS.201608-658ST.

[6] F. Q. AL-Khalidi, R. Saatchi, D. Burke, H. Elphick, and S. Tan, "Respiration rate monitoring methods: A review," *Pediatr. Pulmonol.*, vol. 46, no. 6, pp. 523–529, 2011, doi: 10.1002/ppul.21467.

[7] A. Siqueira, A. F. Spirandeli, R. Moraes, and V. Zarzoso, "Respiratory waveform estimation from multiple accelerometers: An optimal sensor number and placement analysis," *IEEE J. Biomed. Health Inform.*, vol. 23, no. 4, pp. 1507–1515, 2018, doi: 10.1109/JBHI.2018.2851030.

[8] A. Gaidhani, K. S. Moon, Y. Ozturk, S. Q. Lee, and W. Youm, "Extraction and analysis of respiratory motion using wearable inertial sensor system during trunk motion," *Sensors*, vol. 17, no. 12, pp. 1–12, 2017, doi: 10.3390/s17122932.

[9] Y. Jiang, "Power generation humidity sensor based on NaCl/halloysite nanotubes for respiratory patterns monitoring," *Sens. Actuators B Chem.*, vol. 380, no. 1, pp. 1–12, 2023, doi: 10.1016/j.snb.2023.133396.

[10] Z. Liu, "Flexible piezoelectric nanogenerator in wearable self-powered active sensor for respiration and healthcare monitoring," *Semicond. Sci. Technol.*, vol. 32, no. 6, pp. 1–12, 2017, doi: 10.1088/1361-6641/aa6c58.

[11] E. J. Pino, B. Gómez, E. Monsalve, and P. Aqueveque, "Wireless Low–Cost Bioimpedance Measurement Device for Lung Capacity Screening," in Proc. 2019 41st Annu. *Int. Conf. IEEE Eng. Med. Biol. Soc. (EMBC)*, Berlin, Germany, vol. 2019, no. 1, pp. 1187–1190, doi: 10.1109/EMBC.2019.8857766.

[12] U. Z. George, K. S. Moon, and S. Q. Lee, "Extraction and analysis of respiratory motion using a comprehensive wearable health monitoring system," *Sensors*, vol. 21, no. 4, pp. 1393-1403, 2021, doi: 10.3390/s21041393.

[13] E. Helfenbein, R. Firoozabadi, S. Chien, E. Carlson, and S. Babaeizadeh, "Development of three methods for extracting respiration from the surface ECG: A review," *J. Electrocardiol.*, vol. 47, no. 6, pp. 819–825, 2014, doi: 10.1016/j.jelectrocard.2014.07.020.

[14] F. Yasuma and J. Hayano, "Respiratory sinus arrhythmia: Why does the heartbeat synchronize with respiratory rhythm?," *Chest*, vol. 125, no. 2, pp. 683–690, 2004, doi: 10.1378/chest.125.2.683.

[15] P. H. Charlton, T. Bonnici, L. Tarassenko, D. A. Clifton, R. Beale, and P. J. Watkinson, "An assessment of algorithms to estimate respiratory rate from the electrocardiogram and photoplethysmogram," *Physiol. Meas.*, vol. 37, no. 4, pp. 610–626, 2016, doi: 10.1088/0967-3334/37/4/610.

[16] J. Lázaro, "Electrocardiogram derived respiratory rate using a wearable armband," *IEEE Trans. Biomed. Eng.*, vol. 68, no. 4, pp. 1056–1065, 2020, doi: 10.1109/TBME.2020.3012731.

[17] T. Penzel, "Modulations of heart rate, ECG, and cardio-respiratory coupling observed in polysomnography," *Front. Physiol.*, vol. 7, no. 1, pp. 460-472, 2016, doi: 10.3389/fphys.2016.00460.

[18] C. Varon, "A comparative study of ECG-derived respiration in ambulatory monitoring using the single-lead ECG," *Sci. Rep.*, vol. 10, no. 1, pp. 5704-5716, 2020, doi: 10.1038/s41598-020-62670-3.

[19] Z. Zhang, J. Zheng, H. Wu, W. Wang, B. Wang, and H. Liu, "Development of a respiratory inductive plethysmography module supporting multiple sensors for wearable systems," *Sensors*, vol. 12, no. 10, pp. 13167–13184, 2012, doi: 10.3390/s121013167.

[20] E. Piuzzi, S. Pisa, E. Pittella, L. Podestà, and S. Sangiovanni, "Low-cost and portable impedance plethysmography system for the simultaneous detection of respiratory and heart activities," *IEEE Sens. J.*, vol. 19, no. 7, pp. 2735–2746, 2018, doi: 10.1109/JSEN.2018.2883466.

[21] J. Niu, M. Cai, Y. Shi, S. Ren, W. Xu, W. Gao, Z. Luo, and J. M. Reinhardt, "A novel method for automatic identification of breathing state," *Sci. Rep.*, vol. 9, no. 1, pp. 1–12, 2019, doi: 10.1038/s41598-018-36733-w.

[22] M. Chatterjee, A. Pramanik, and S. Mitra, "Multimodal wearable sensor system for real-time monitoring of cardiac and respiratory activities," *IEEE Sens. J.*, vol. 21, no. 14, pp. 15885–15894, 2021, doi: 10.1109/JSEN.2021.3072783.

[23] D. J. Doyle, "Acoustical respiratory monitoring in the time domain," *Open Anesth*. J., vol. 13, no. 1, pp. 144–151, 2019, doi: 10.2174/2589645801913010144.

 ISSN 2723-6471

[24] M. E. Chowdhury, A. Khandakar, K. Alzoubi, S. Mansoor, A. M. Tahir, M. B. I. Reaz, and N. Al-Emadi, "Real-time smart-digital stethoscope system for heart diseases monitoring," *Sensors*, vol. 19, no. 12, pp. 1–12, 2019, doi: 10.3390/s19122781.

[25] M. Faezipour and A. Abuzneid, "Smartphone-based self-testing of COVID-19 using breathing sounds," *Telemed. e-Health*, vol. 26, no. 9, pp. 1202–1205, 2020, doi: 10.1089/tmj.2020.0091.

[26] J. Niu, Y. Shi, M. Cai, Z. Cao, D. Wang, Z. Zhang, and X. D. Zhang, "Detection of sputum by interpreting the time-frequency distribution of respiratory sound signal using image processing techniques," *Bioinformatics*, vol. 34, no. 5, pp. 820–827, 2018, doi: 10.1093/bioinformatics/btx660.

[27] G. Tyulepberdinova, Z. Oralbekova, M. Kunelbayev, G. Amirkhanova, and S. Issabayeva, "Design of an IoT-enabled wearable device for stress level monitoring," *Int. J. Innov. Res. Sci. Stud*., vol. 8, no. 1, pp. 599–612, 2025, doi: 10.53894/ijirss.v8i1.4406.

[28] I. Frerichs, B. Vogt, J. Wacker, "Multimodal remote chest monitoring system with wearable sensors: a validation study in healthy subjects," *Physiol. Meas*., vol. 41, no. 1, 015006, pp. 1-20, 2020, doi: 10.1088/1361-6579/ab668f.

[29] J. A. Sanchez-Perez, J. A. Berkebile, B. N. Nevius, "A wearable multimodal sensing system for tracking changes in pulmonary fluid status, lung sounds, and respiratory markers," *Sensors*, vol. 22, no. 3, article 1130, pp. 1-12, 2022, doi: 10.3390/s22031130.